Fault tolerant control of a three-phase three-wire shunt active filter system based on reliability analysis

Philippe Poure, Philippe Weber, Didier Theilliol, Shahrokh Saadate

▶ **To cite this version:**

Philippe Poure, Philippe Weber, Didier Theilliol, Shahrokh Saadate. Fault tolerant control of a three-phase three-wire shunt active filter system based on reliability analysis. Electric Power Systems Research, 2009, 79 (2), pp.325-344. ⟨10.1016/j.epsr.2008.07.003⟩. ⟨hal-00347005⟩

HAL Id: hal-00347005

https://hal.science/hal-00347005v1

Submitted on 10 Feb 2022

HAL is a multi-disciplinary open access archive for the deposit and dissemination of scientific research documents, whether they are published or not. The documents may come from teaching and research institutions in France or abroad, or from public or private research centers.

L'archive ouverte pluridisciplinaire **HAL**, est destinée au dépôt et à la diffusion de documents scientifiques de niveau recherche, publiés ou non, émanant des établissements d'enseignement et de recherche français ou étrangers, des laboratoires publics ou privés.

HAL Authorization

Fault tolerant control of a three-phase three-wire shunt active filter system based on reliability analysis

P. POURE*, P. WEBER°, D. THEILLIOL° and S. SAADATE[+]

°Centre de Recherche en Automatique de Nancy UMR 7039, Nancy-Universite, CNRS
*Laboratoire d'Instrumentation Electronique de Nancy EA 3440, Nancy-Universite,
[+]Groupe de Recherches en Electrotechnique et Electronique de Nancy UMR 7037 , Nancy-Universite, CNRS
Faculté des Sciences et Techniques - BP 239 - 54506 Vandoeuvre Cedex France
Tel: (33) 383 684 160 - Fax: (33) 383 684 153

philippe.poure@lien.uhp-nancy.fr, philippe.weber@cran.uhp-nancy.fr,
didier.theilliol@cran.uhp-nancy.fr, shahrokh.saadate@green.uhp-nancy.fr

Corresponding author: P. POURE
Laboratoire d'Instrumentation Electronique de Nancy
LIEN, EA 3440, Nancy-University
Faculté des Sciences et Techniques - BP 239 - 54506 Vandoeuvre Cedex France
Tel: (33) 383 684 160 - Fax: (33) 383 684 153
Email : philippe.poure@lien.uhp-nancy.fr

Abstract

This paper deals with fault tolerant shunt three-phase three-wire active filter topologies for which reliability is very important in industry applications. The determination of the optimal reconfiguration structure among various ones with or without redundant components is discussed based on reliability criteria. First, the reconfiguration of the inverter is detailed and a fast fault diagnosis method for power semi-conductor or driver fault detection and compensation is presented. This method avoids false fault detection due to power semi-conductors switching. The control architecture and algorithm are studied and a fault tolerant control strategy is considered. Simulation results in open and short circuit cases validate the theoretical study. Finally, the reliability of the studied three-phase three-wire filter shunt active topologies is analyzed to determine the optimal one.

Keywords: Reliability analysis, Fault tolerant control, active filter, fault detection, fault compensation.

Introduction

The reliability of power electronic equipments becomes extremely important in industry applications. The fault mode behaviour of static converters, protection and fault tolerant control of voltage source inverter systems has been covered in a large number of publications in the specific literature. Most of them are focused on induction motor drive applications. Kastha and Bose considered various fault modes of a voltage source Pulse Width Modulation (PWM) inverter system for induction motor drive [1]. They have studied rectifier diode short circuit, inverter transistor base driver open and inverter transistor short-circuit conditions. However, they do not propose to reconfigure the inverter topology. Thybo was interested in fault tolerant control of induction motor drive applications using analytical redundancy, providing solutions to most frequent occurring faults [2]. Da Silva *et al.* investigated fault detection of open-switch damage in voltage source PWM motor drive systems [3]. The authors mainly focused the study on detection and identification of the power switch in which the fault has occurred. In another paper, the utilization of a two-leg based topology is investigated when one of the inverter legs is lost [4]. Then, the machine operates with only two stator windings and the PWM control is modified to allow continuous operation of the drive. More recently, four-wire active filter in open phase case is studied in [5], [6] and the authors propose to reconfigure the PWM controler.

Moreover, most conventional control systems or controllers are designed for fault-free systems without taking into account the possibility of fault occurrence. To overcome these limitations, modern complex systems use sophisticated controllers which are developed with fault accommodation and tolerance capabilities, to perform reliability and performance requirements. The Fault Tolerant Control (FTC) system is a control system that can maintain system performance closely to the desirable one and preserves stability conditions, not only when the system is in fault-free case but also in the presence of faulty component, or at least ensures degraded performances, which can be accepted as a trade-off. FTC has been motivated by different goals for different applications; it could improve reliability and safety in industrial processes and safety-critical applications such as flight control and nuclear power plant operation [7]. Various studies on FTC are based on hardware or analytical redundancy. The hardware redundancy technique consists of switching from the failed part of the process to another achieving the same task. The analytical redundancy is an alternative to solve the FTC problem avoiding the disadvantages of the hardware redundancy such as high cost and space.

This paper deals with fault tolerant three-phase three-wire shunt active filter topologies. The determination of the optimal reconfiguration structure among various ones with or without redundant components is discussed. The fault tolerant system architecture is presented in section II. The section three presents the studied fault tolerant active filter topologies. The reconfiguration of the inverter is first detailed. Then, a fast and reliable fault diagnosis method for power semi-conductor or driver fault detection is presented in section four. This optimised detection method avoids false fault detection due to power semi-conductors switching. More, it allows to compensate the fault as fast as possible, after the fault occurrence, and consequently avoids a secondary fault. The next section describes the control architecture and algorithm. In the section six, the reliability of the three-phase three-wire shunt active filter topologies is analyzed. Based on the highest reliability criterion, the optimal structure is determined in order to achieve desired objectives as close as possible to nominal ones. The application results are presented before the conclusion and perspectives.

I. Fault tolerant system architecture

Let us define the control problem by the triplet $< \gamma_g , C, U >$, in the spirit of Staroswiecki [8], where:

- γ_g Global objectives
- C A set of constraints given by the structure of system S_m, and the parameters of closed-loop system θ
- U A set of control laws

In fault-free case, this problem could be solved by defining a control law $u \in U$, such that the controlled system achieves the global objectives γ_g under structure S_m and parameters θ constraints. It is assumed that nominal global objectives γ_g^{nom} are achieved under a nominal control law u_{nom} and a nominal structure S_{nom} which uses some sub-systems. The fault occurrence is supposed to modify the structure S_{nom} for which the objectives can be or can not be achieved under a new structure.

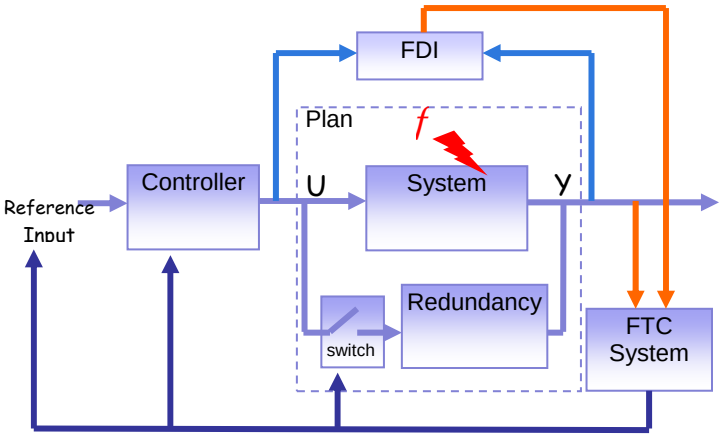

Fig. 1: Global FTC system architecture.

The FTC problem is then defined by $< \gamma_g, C, U >$, which has a solution that could achieve γ_g^{nom} by changing the structure, parameters and/or control law of the post-fault system. Fig. 1 presents the global architecture of FTC system with ability of disconnection or replacement of faulty sub-systems. In some cases, no solution may exist, and then global objectives must be redefined to the degraded ones, denoted as γ_g^d.

Under assumptions that there exist several structures S_m $m = (1, \ldots, M)$, the problem statement is formulated by the following question: how to choose the optimal structure in the sense that for a given criterion J the chosen structure can maintain the objectives γ_g^{nom}? An answer will be provided in [9] based on reliability analysis.

Compared to Guenab *et al.* [9], and due to the specific application, the present paper proposes a reliability analysis studied off-line. Some publications have introduced reliability analysis for fault tolerant control systems. Also Staroswiecki *et al.* [8] have proposed a sensor reconfiguration based on physical redundancy where the reliability analysis provided some information to select the optimal redundant sensors. In [10] and [11], Markov models are used to estimate the system reliability where it is supposed that the sub-systems take two states: intact (available) or failed (unavailable) [12], [13].

II. Fault tolerant active filter topologies

The classical three-leg shunt power active filter topology is depicted in Fig. 2. It is composed by a grid (e_{si} for i = {1, 2, 3}), a non-linear load and a voltage source inverter. The non-linear load consists in a three-phase diode rectifier feeding (R, L) load. The grid is balanced with series resistances r_s and inductances l_s for each phase. The power converter is a voltage source inverter with equal series resistances r_f and inductances l_f for each phase.

To ensure filtering, the shunt active filter output currents are controlled to provide in real time reactive power and harmonic currents generated by the non-linear load. The capacitor C_{dc} is an energy storage capacity.

In this paper, we studied two fault tolerant shunt active filter topologies. These fault tolerant topologies use connecting devices (triacs T_{ri}) and fuses f_i. They allow reconfiguring the power converter topology after fault detection in power switch or driver failure case. These topologies are based on the classical and "healthy" topology τ_0 presented in Fig. 2 [14].

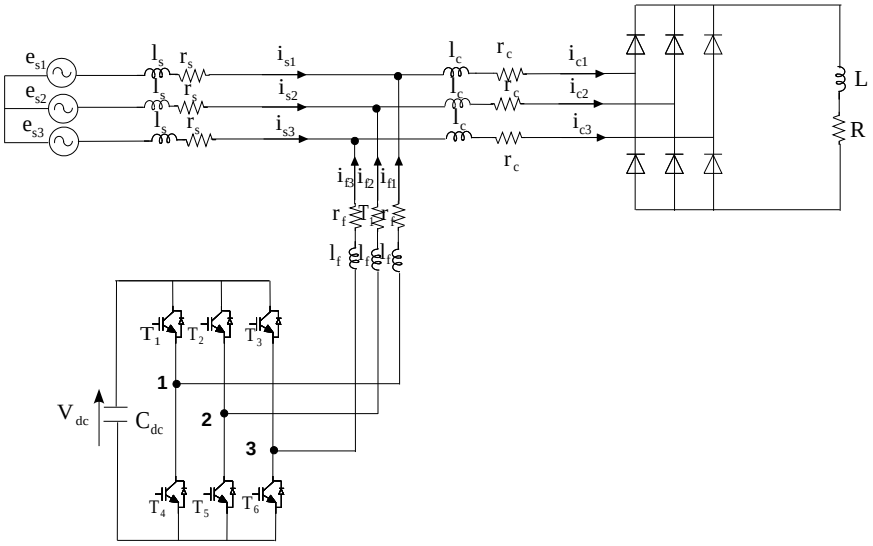

Fig. 2: Classical three-leg shunt active filter topology τ_0.

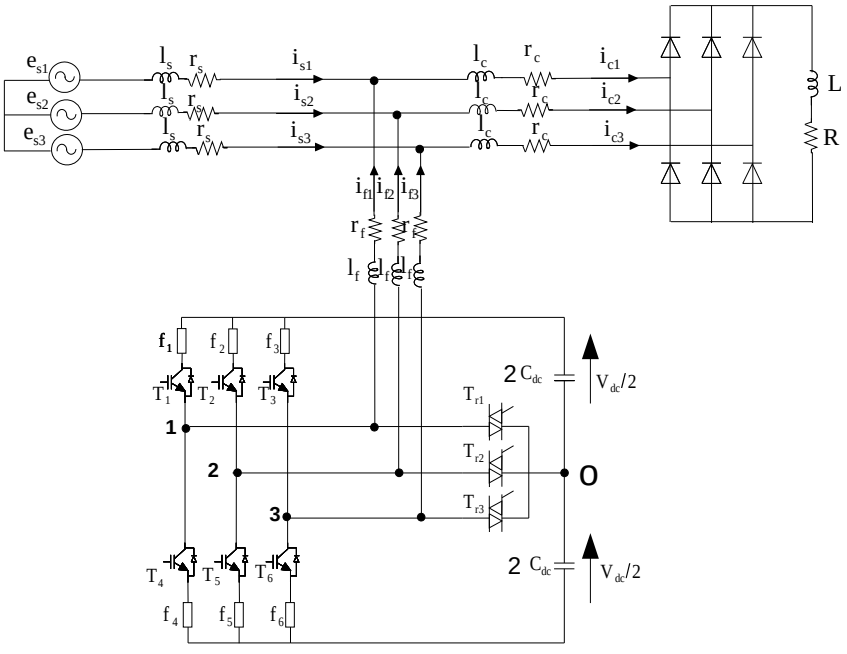

Fig. 3: Fault tolerant three-leg shunt active filter topology τ_1.

The fault tolerant three-leg topology, depicted in Fig. 3 is first studied. The three legs are used in "healthy" condition. This structure τ_1 includes bi-directional devices T_{rk} (k = {1, 2, 3}), triacs in this case to simplify control. These triacs allow connecting the inverter faulty phase number k to the middle point O of the capacitors. By this way, for the leg number k, if one of the semi-conductor T_i or

its associated driver is faulty, the leg including T_i is isolated and the point *k* is directly connected to the capacitor middle point O by switching on the suited triac T_{rk}. Consequently, the post fault topology becomes a two-leg structure with the faulty phase directly connected to the point O. The fault free case leads to the nominal structure $S_{nom}^{\tau_1}$ and the three bi-directional devices lead to three structures $S_1^{\tau_1}$, $S_2^{\tau_1}$ and $S_3^{\tau_1}$ allowing the tolerance of T_i faults. Then four structures are available with the topology τ_1 which are presented in Fig. 4.

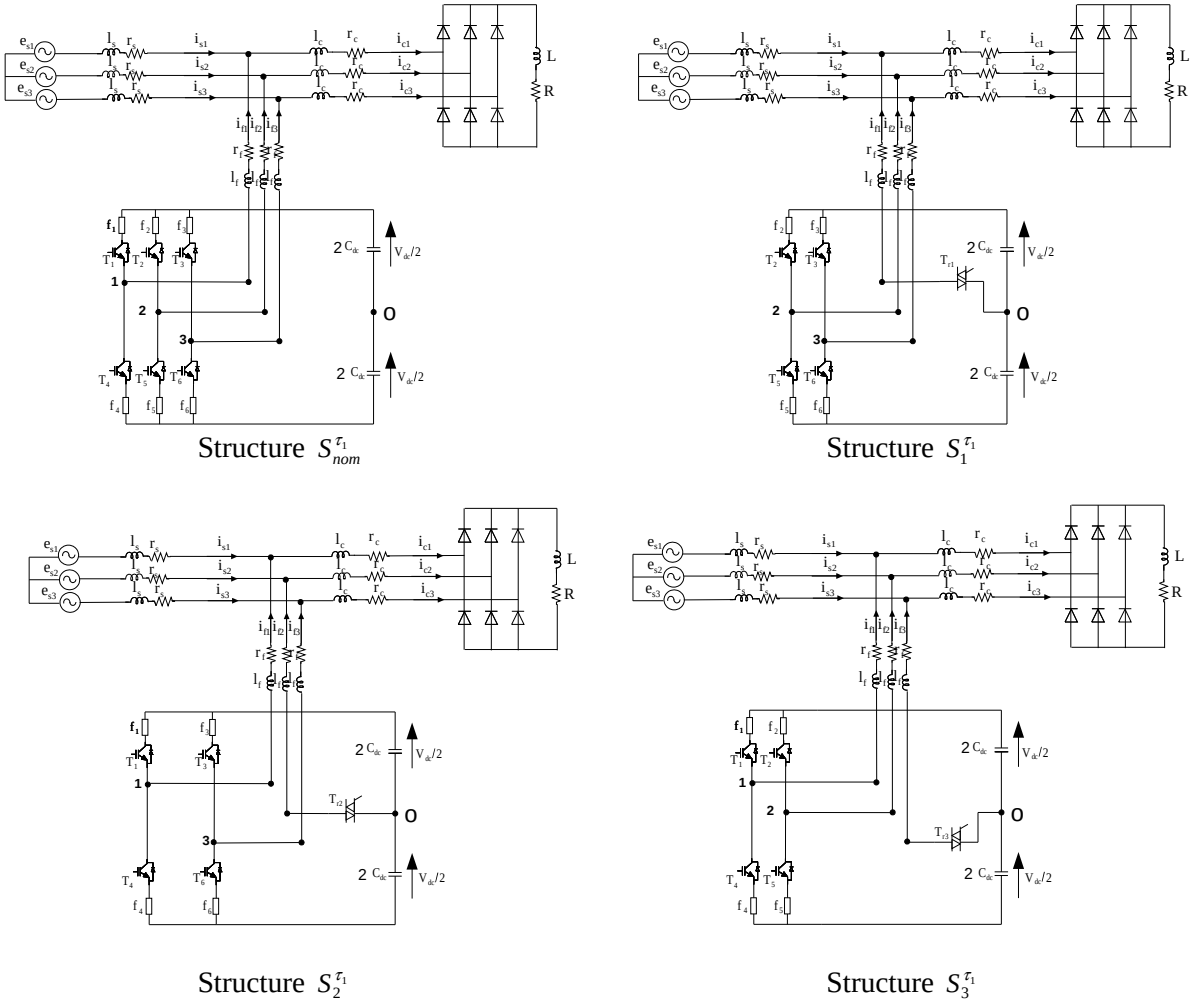

Fig. 4: Four structures from the topology τ_1.

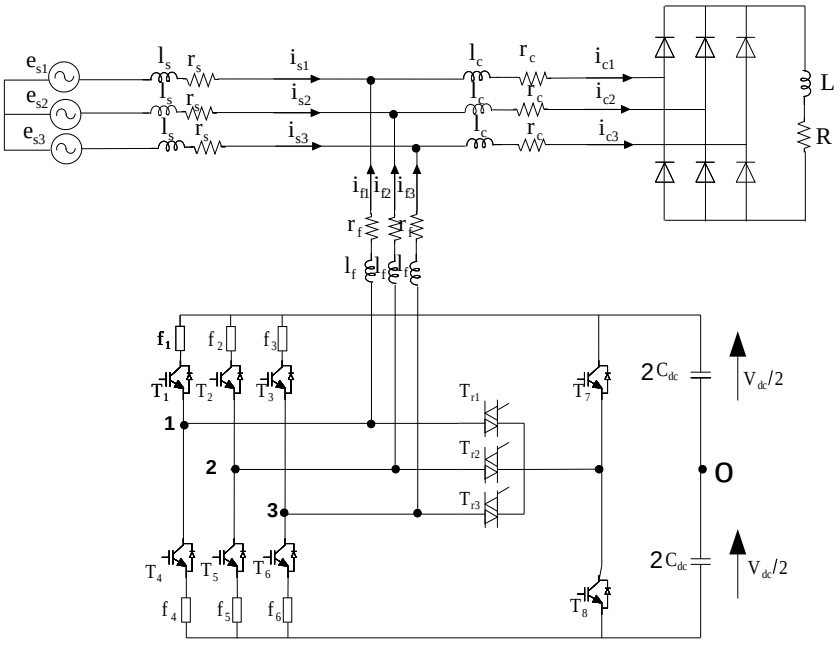

Fig. 5: Fault tolerant four-leg shunt active filter topology τ_2.

The second topology τ_2 is a four-leg active filter, presented in Fig. 5. Here, the use of two capacitors is mandatory to be able to measure the pole voltages v_{kO} (k = 1, 2, 3), necessary for the fault diagnosis. The fourth redundant leg is composed of T_7 and T_8 devices. If necessary, this leg will replace the faulty one. Bi-directional devices allow connecting the faulty phase number k to the redundant leg. After fault detection, the three filter structures $S_1^{\tau_2}$, $S_2^{\tau_2}$ and $S_3^{\tau_2}$ remain similar to the structure $S_{nom}^{\tau_2}$, the classical three-leg topology presented in Fig. 2.

In summary, in a failure case for the leg number k, the following steps achieve the compensation [14]:
- detection of the faulty switch or driver of the leg number k;
- removing the commands of the two drivers of the leg number k;
- connecting the faulty DC side phase k to the point O of the capacitor energy storage (topology τ_1) or replacing the faulty leg by the redundant one (topology τ_2);
- applying the suited post-fault control strategy.

III. Fault diagnosis and reconfiguration method

Power semi-conductors or drivers fault detection is based on the comparison between measured and estimated pole voltages v_{kO} (k = 1, 2, 3), respectively noted v_{kOm} and v_{kOes}. The estimated voltages can be expressed by:

$$v_{kOes} = (2 \times \delta_k - 1) \times \frac{v_{dc}}{2} \tag{1}$$

Where δ_k = {0, 1} is the switching pattern of the top semi-conductor of the leg number k and v_{dc} is the dc-link voltage. The fault occurrence can be determined by analysing the voltage error obtained from the difference between the measured and estimated pole voltages. This voltage error is given by:

$$\varepsilon_{kO} = v_{kOm} - v_{kOes} \tag{2}$$

If we suppose that the switches are ideal, the measured and estimated pole voltages are equal in normal operation and thus their difference is zero. Thus, assuming ideal switches, the fault occurrence in each leg can be determined with a comparator that compares the measured and estimated pole

voltages. However, in real case, because of turn-off and turn-on propagation time and interlock dead time generated by the drivers, the voltage error is not equal to zero and contains some picks during switching time.

To avoid false fault detection due to power semi-conductors switching, we think of transforming the "voltage" signal ε_{kO} (t) in a "time" signal int_{kO} (t). From signal $\varepsilon_{kO}(t)$, we defined a signal $int_{kO}(t)$, constituted of picks having as maximal value the time during which $\varepsilon_{kO}(t)$ is different from zero [14].

IV. Active filter control: Topologies and global objective

The fault tolerant topology τ_1 is a three-leg structure. The three legs are used in healthy condition $S_{nom}^{\tau_1}$. The post-fault topology τ_1 leads to two-leg structures, $S_1^{\tau_1}$ $S_2^{\tau_1}$ or $S_3^{\tau_1}$, with faulty phase connected to the point O. The four-leg fault tolerant topology τ_2 is based on hardware redundancy; only three legs are used in the same time in the structures which are $S_{nom}^{\tau_2}$, $S_1^{\tau_2}$, $S_2^{\tau_2}$, or $S_3^{\tau_2}$.

Moreover, the same shunt active filter control is available for three-leg and two-leg structures [14]. The major advantage of the control law $u \in U$ is to be suitable for the set of fault-free structure $S_{nom}^{\tau_1}$ and $S_{nom}^{\tau_2}$ and the set of the faulty structures: $S_m^{\tau_1}$ and $S_m^{\tau_2}$ for $m = (1,\ldots,M)$.

According to this control scheme, the same reference voltage V_{dcref} can be used for the fault free case of the topology τ_1 and the fault tolerant four-leg shunt active filter, topology τ_2. The reconfigured structure is equivalent to the fault-free case $S_{nom}^{\tau_1}$. However, concerning the fault tolerant three-leg shunt active filter (topology τ_1), the structure is initially composed of three legs and becomes a two-leg topology after reconfiguration. The V_{dcref} value must be changed or not after reconfiguration simultaneously with converter reconfiguration, depending on its value in healty conditions. If the V_{dcref} value in healty conditions is not equal to the suited value in reconfigured mode (1400V in our application case), it must be changed and the new V_{dcref} value should be twice larger than in fault-free case (700V in our case) [14].

Fig. 6 presents the block diagram for the active filter control. The major advantage of this control principle is to be suited for any structure. The task of this control is to determine the harmonic current references to be generated by the active filter. The current references are identified using a modified version of instantaneous active and reactive power method proposed by Akagi [15], associated with two digital voltage and current high selectivity filters, first studied by Song [16]. The active filter control principle is detailed in [14].

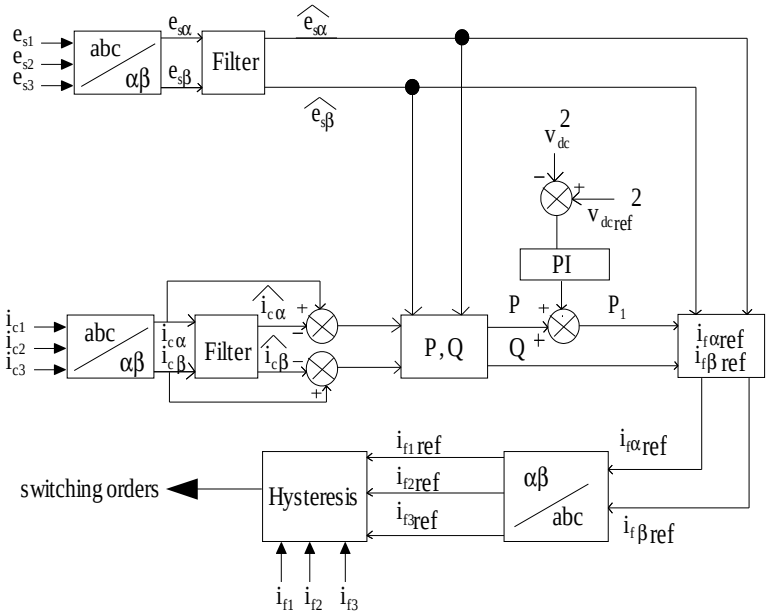

Fig. 6: Active filter control.

As presented in this paper, various shunt three phase active filter topologies and reconfiguration structures can be considered in faulty cases with a classical hardware redundancy or suitable structures with $\gamma_g = \gamma_g^{nom}$ for the same control law $u \in U$, $\forall\ S_m$ $m = (1,\ldots,M)$ structures. Consequently, the fault tolerant control problem $< \gamma_g, C, U >$ could be summarized by determining the optimal structure with the highest reliability.

According to the dynamic behaviour of the current and voltage system (see simulation results in section VI), it can be noticed that with a classical hardware redundancy or suitable structure (i.e. $\forall\ S_m$ $m = (1,\ldots,M)$ structures), the reconfigured structure provides a global objective $\gamma_g = \gamma_g^{nom}$ for the same control law $u \in U$. The global objective consists in guaranteeing for the grid currents a Total Harmonic Distorsion (THD) value lower than 5%, before and after fault occurrence.

V. Reliability analysis

Representing system failure in a probabilistic way is attractive because it naturally accounts the uncertainty. To make such representation, the process behaviour is considered as a random variable that takes its values from a finite state space corresponding to the possible process states. A discrete time stochastic process models deterioration. In the case of finite or countable state space, Markov processes are represented by a graphic called Markov Chain (MC) [17].

Markov Chain models a sequence of random variables $\{X_k,\ k = 0, 1, 2...\}$ for which the Markovian property is held. Let $\{\eta_1,...,\eta_M\}$ be a finite set of the possible mutually-exclusive states of each X_k. The probability distribution over these states is represented by the vector $p(X_k)$:

$$p(X_k) = \left[p(X_k = \eta_1),...p(X_k = \eta_m),...,p(X_k = \eta_M)\right]$$

$$\text{with } \sum_{m=1}^{M} p(X_k = \eta_m) = 1 \qquad (3)$$

In this paper, only constant failure rates are considered. Homogenous Markov chains are used for this case because of the stationarity of transition probabilities. In such model, transition probabilities are time invariant and depend only on values states:

$$p_{ij} = p(X_{k+1} = \eta_i \mid X_k = \eta_j) = p(X_{k+2} = \eta_i \mid X_{k+1} = \eta_j) \tag{4}$$

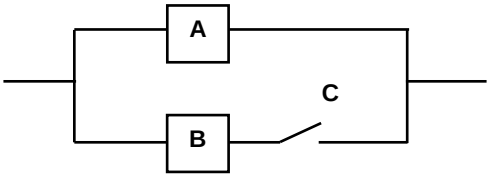

Fig. 7: Reliability block diagram of passive redundancy.

In a homogeneous discrete-time MC, the transition matrix $\mathbf{P}_{MC}$ between the states is defined from failure rate parameters. For instance, let us consider the passive redundancy system (Fig. 7). The MC is presented in Fig.8 with three states {1, 2, 3}, then the transition matrix is defined as:

$$\mathbf{P}_{MC} = \begin{bmatrix} 1 - p_{12} + p_{13} & p_{12} & p_{13} \\ 0 & 1 - p_{23} & p_{23} \\ 0 & 0 & 1 \end{bmatrix} \tag{5}$$

Where

- $p_{12} \cong \lambda_A \cdot (1-\rho) \cdot \Delta t$: λ_A is a constant failure rate of the component A; ρ is the commutation failure probability and Δt is the time interval. The probability p_{12} can be interpreted as the probability that the component A fails after the time Δt and the commutation on the component B is successful.
- $p_{13} \cong \lambda_A \cdot \rho \cdot \Delta t$ is the probability that the component A fails after the time Δt and the commutation on the component B is not successful.
- $p_{23} \cong \lambda_B \Delta t$: λ_B is a constant failure rate of the component B. The probability p_{23} is the probability that the component B fails after the time Δt.

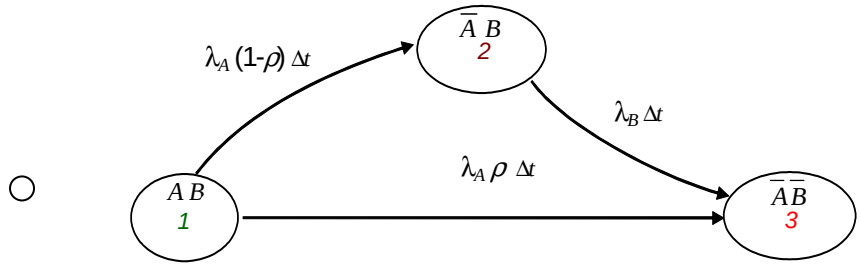

Fig. 8: Markov Chain modelling deterioration of passive redundant system.

Given an initial distribution over states $p(X_0)$, the probability distribution over states after k stage $p(X_k)$ is obtained from the Chapman-Kolmogorov equation:

$$p(X_k) = p(X_0) \prod_{i=0}^{K} \mathbf{P}_{MC} \tag{6}$$

Assuming that $i \in \{1...l\}$ represents the functioning states, system reliability is defined as:

$$R(k) = \sum_{i \in \{1...l\}} p(X_k = s_i) \tag{7}$$

The application of eq. 7 to the Markov model fig. 8 gives:

$$R(k) = \sum_{i \in \{1...2\}} p(X_k = s_i) = p(X_k = s_1) + p(X_k = s_2) \tag{8}$$

The use of classic MC to model deterioration in systems needs to enumerate all possible states that lead sometimes to a huge transition matrix. Aggregation of states is used to decrease the complexity of the model if several components have exactly the same parameters. The illustration of this simplification is given in the Fig. 9 to model the topology τ_0 presented in Fig. 2.

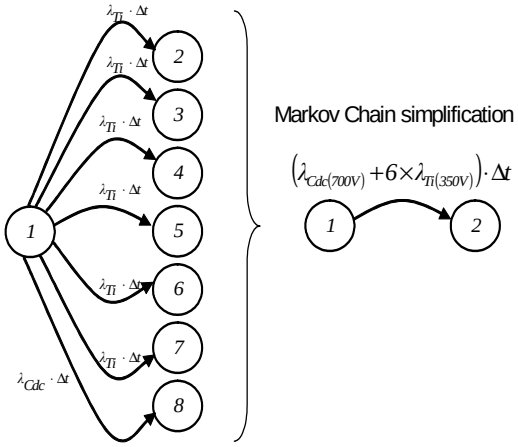

Fig. 9: Markov Chain simplification of the topology τ_0 model.

VI. Simulation results and comments

This section presents simulation results obtained with Matlab simulator for the two active filter topologies studied. Simulation parameters are given in Table 1. The hysteresis band is equal to 20 A.

Mains line voltage	400 V
Mains frequency	50 Hz
Mains inductance (L_s)	0.1 mH
Mains resistance (R_s)	0.2 mΩ
Load ac inductor (L_c)	15 µH
Load ac resistance (R_c)	0.4 mΩ
Active filter inductance (L_f)	150 µH
Load inductor (L)	2.5 mH
Load resistance (R)	0.6 Ω
DC capacitor (C_{dc})	17.6 mF

Table 1. Simulation parameters.

A. Case of the three-leg topology τ_1

Fig. 10 presents simulation results in an open circuit case. We simulated the fault on the top switch of the leg number 3, introduced at *t* = 80 ms. The value of the capacitor voltage reference V_{dc}^{ref} is set to 1400V before and after fault. Results presented in Fig.10 show that proposed fault tolerant system preserved the main performance features after fault compensation. The mean switching frequency is equal to 9.1 kHz before fault with the structure $S_{nom}^{\tau_1}$ and equal to 9.6 kHz after fault with the structure $S_3^{\tau_1}$. The THD is equal to 1.1 % before fault with the structure $S_{nom}^{\tau_1}$ and equal to 1.6 % after fault with the structure $S_3^{\tau_1}$.

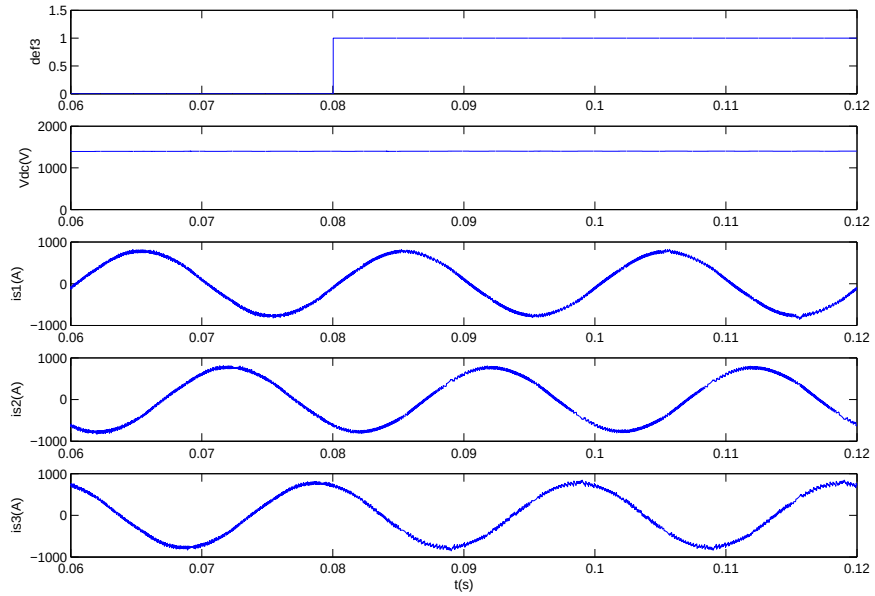

Fig. 10: Case of an open circuit with a unique reference voltage V_{dc}^{ref} =1400 V.

Fig. 11 presents results in an open circuit case. We simulated the fault of the top switch of the leg number 3, introduced at t=80 ms. The value of the capacitor voltage reference V_{dc}^{ref} is set to 700 V before fault and to 1400 V after fault detection and compensation. The proposed fault tolerant system preserved the main performance features after fault compensation with the structure $S_3^{\tau_1}$. More, the mean switching frequency is equal to 3.7 kHz before fault with the structure $S_{nom}^{\tau_1}$ and equal to 9.6 kHz after fault with the structure $S_3^{\tau_1}$. The THD is equal to 1.5 % before fault with the structure $S_{nom}^{\tau_1}$ and equal to 1.6 % after fault with the structure $S_3^{\tau_1}$.

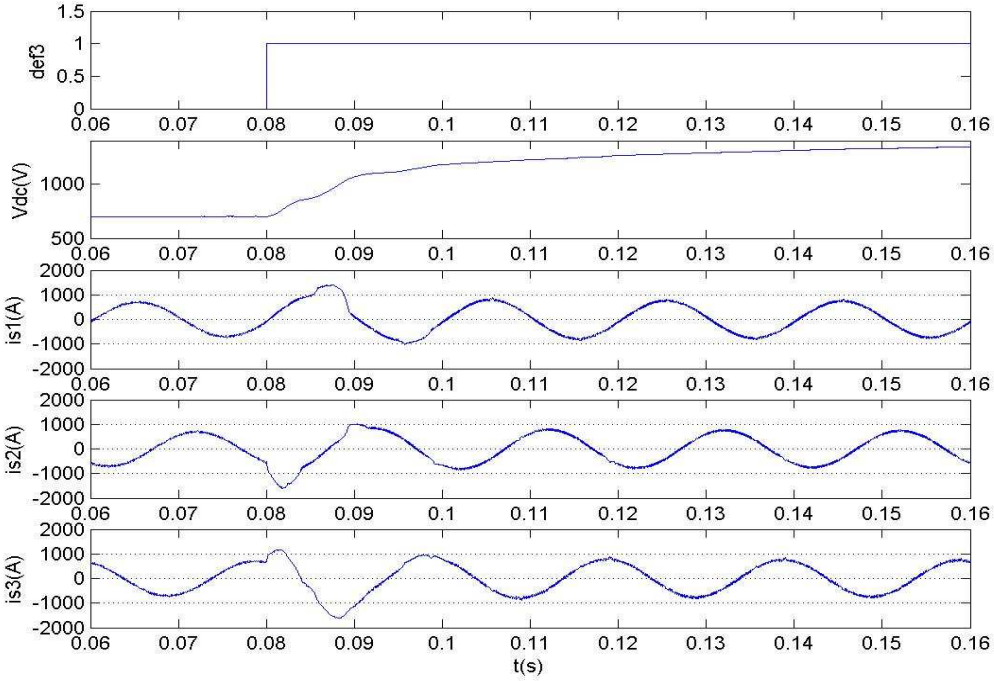

Fig. 11: Case of an open circuit with 2 reference voltages.

B. Case of the four-leg topology τ_2

Fig. 12 presents simulation results in open circuit case. We simulated the fault of the top switch of the leg number 3 introduced at t = 80 ms. The value of the capacitor voltage reference V_{dc}^{ref} is set to 700V. Performances for waveforms Fig. 12 remain the same before the reconfiguration with the structure $S_{nom}^{\tau_2}$ and after the reconfiguration with the structure $S_3^{\tau_2}$. The THD value is equal to 0.9 % and the mean switching frequency equal to 8.7 kHz.

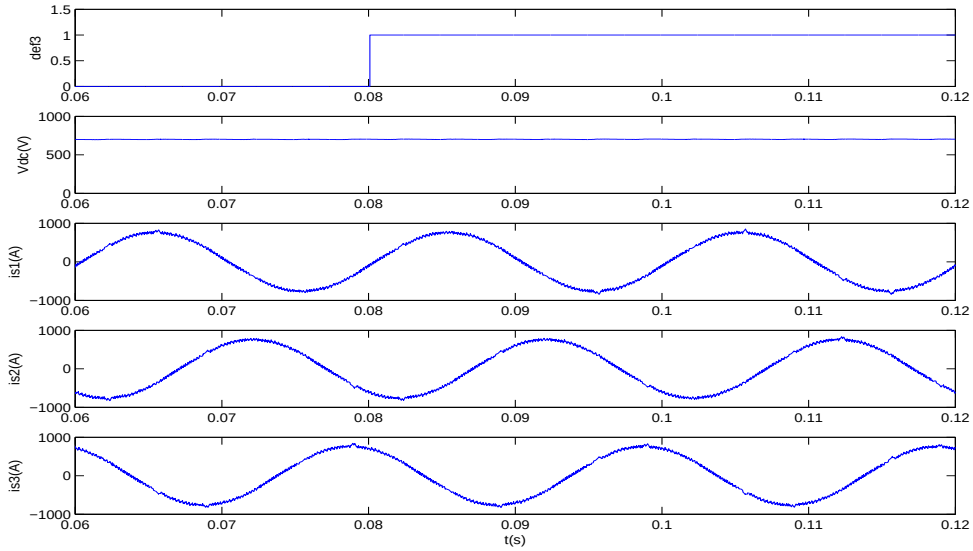

Fig. 12: Case of an open circuit with V_{dc}^{ref} =700 V.

Fig. 13 presents simulation results in a short circuit case. We simulated the fault of the bottom switch of the leg number 3, introduced at t = 80 ms. The value of the capacitor voltage reference V_{dc}^{ref} is set to 700V. The time response of the fuse f_3 is equal to 6 µs. Performances for waveforms Fig. 12 are the same before the reconfiguration with the structure $S_{nom}^{\tau_2}$ and after the reconfiguration with the structure $S_3^{\tau_2}$. The THD value is equal to 0.9 % and the mean switching frequency equal to 8.7 kHz. However, compared with open circuit case, Vdc voltage deacreases up to 650V just after the fault occurrence.

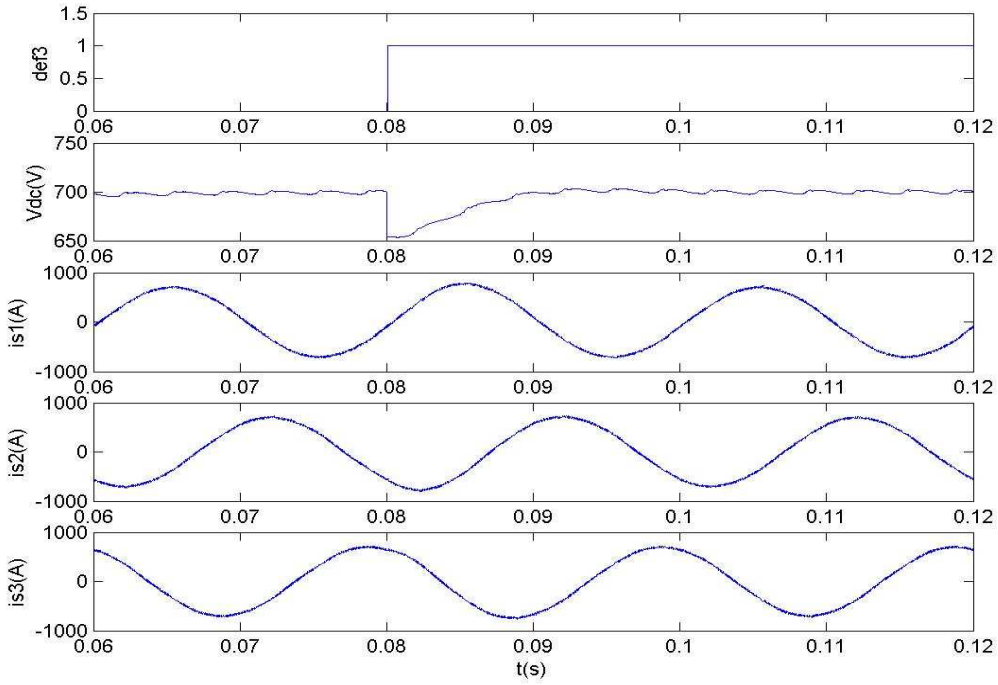

Fig. 13: Case of a short circuit with V_{dc}^{ref} =700 V.

C. Reliability analysis:

The voltage level of the IGBT has an important impact on the reliability of this component because it leads the increasing of the temperature that strongly impacts the failure rate [18]. Due to the fact that the temperature increases when the voltage increases, let us consider that the failure rates of T_i increase: $\lambda_{Ti(350V)} < \lambda_{Ti(700V)}$; and, the failure rate of the capacitor increase with the voltage: $\lambda_{Cdc(350V)} < \lambda_{Cdc(700V)}$.

The following table 2 presents the value of the failure rate of the components according to the voltage and the Mean Time To Failure (MTTF). The $\lambda_{Ti(noUsed)}$ represents the failure rate of the IGBT of the redundant leg when the IGBT are not used in commutation by the driver; λ_{fuz} is the failure rate of the fuses f_i, $\lambda_{Triac(OpenCircuit)}$ et $\lambda_{Triac(ShortCircuit)}$ represent the failure rate of the triacs with an Open Circuit failure when the triac is normally closed, and Short Circuit failure when the triac is normally open, respectively. The variable ρ (see Table 3) represents the switched failure probability of the triacs T_{rk}. The parameters of table 2 are chosen according to the values defined in the papers [18], [19] and [20]. These papers describe more particularly specific reliability analysis of IGBT, Thyristor, Fuses and Capacitors.

	Failure rates (/h)	MTTF (h)
$\lambda_{Ti(noUsed)}$	1.51E-06	662 256
$\lambda_{Ti(350V)}$	2.32E-06	431 868
$\lambda_{Ti(700V)}$	2.04E-05	49 056
$\lambda_{Cdc(350V)}$	6.72E-06	148 920
$\lambda_{Cdc(700V)}$	1.38E-05	72 708
λ_{fuz}	1.14E-06	876 000
$\lambda_{Triac(ShortCircuit)}$	1.43E-06	700 800
$\lambda_{Triac(OpenCircuit)}$	1.43E-06	700 800

Table 2: Failure rates of the elementary components.

	Probability of a switching failure
ρ	12.5 E-05

Table 3: Commutation failure probability of the triacs.

Based on section III and section V, the topology τ_0 and the two reconfigured topology τ_1 and τ_2 are represented as Markov Chain models as illustrated in the Fig. 14, Fig. 15, Fig. 16 and Fig. 17 (for simplicity Δt is considered equal to *1* hour). The state η_1 corresponds to the fault-free state. If a failure occurs on capacitor or on T_i, the system is out of order which corresponds to the state η_2 for the topology τ_0 (see Fig. 14) or η_3 for the reconfigured topologies τ_1 (see Fig. 15 and 16) and η_4 is the failure state for the topology τ_2 (see Fig. 17). In the Fig. 15 and Fig.16 (resp.Fig. 17) the state η_2 represents the state of the system for the reconfigured structures $S_m^{\tau_1}$ (resp. $S_m^{\tau_2}$) with the presence of a failure on T_i. It should be noted that the Fig. 15, Fig. 16 and Fig. 17 include the commutation ability of the three and four legs shunt solutions. In the Fig. 17 the state η_3 models a failure of the redundant component before the reconfiguration.

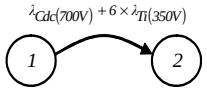

Fig. 14: Markov Chain for modelling the system with the nominal topology τ_0 .

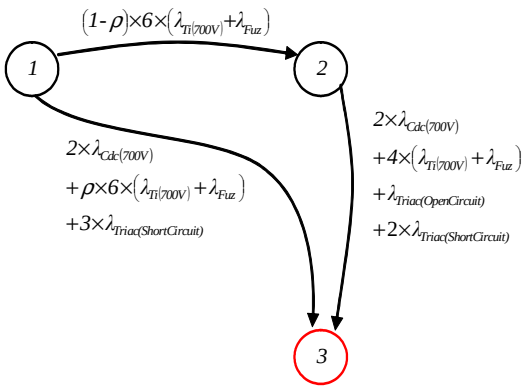

Fig. 15: Markov Chain for topology τ_1 with V_{dcref} = 1400V.

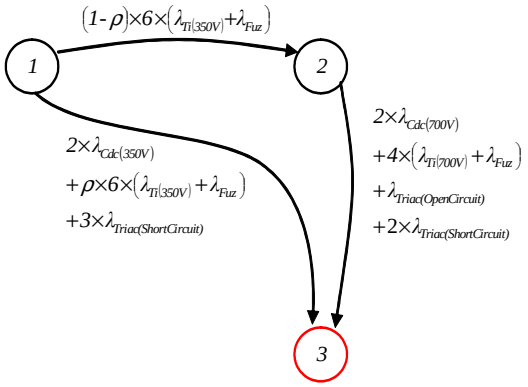

Fig. 16: Markov Chain for topology τ_1 with V_{dcref} = 700V before fault detection and 1400V after.

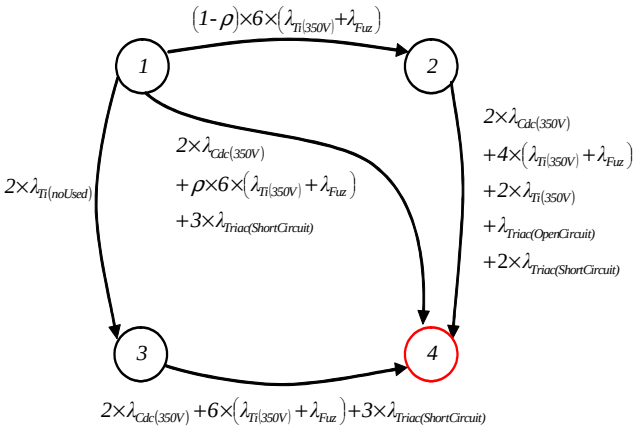

Fig. 17: Markov Chain for modelling the system with four-leg shunt topology τ_2.

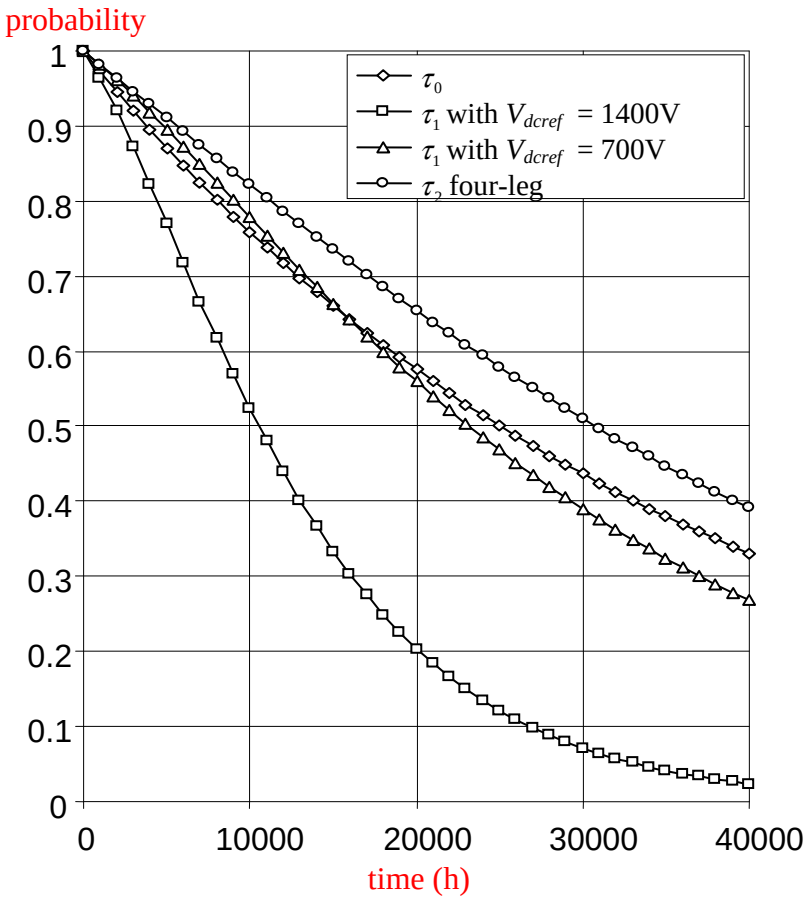

Fig. 18: Reliability computation.

The reliability curves of the systems are shown in Fig. 18. With a hardware redundancy or a suitable topology, the reliability is greater than the initial topology. Moreover, in regard with the parameters, defined in Table 1, the four-leg shunt system is the most efficient topology. Consequently, according to the performance requirements, it is convenient to get the optimal topology as this four-leg topology. Other scalar criteria such as MTTF could be evaluated to choose the topology with the highest reliability. Thank to the Markov model, the MTTF is computed and equal to 36 170 h for the topology τ_0, 13 019 h for the three-leg shunt topology τ_1 with 1400 V before and after the failure occurrence, 30 580 h for the topology τ_1 with V_{dcref} = 700V before fault detection and 1400V after and 39 831 h for the four-leg shunt topology τ_2. The analysis of the MTTF confirms the previous choice: the optimal structure is the four-leg topology.

VII. Conclusion

In this paper, fault tolerant active power filter topologies and associated fault diagnosis method have been studied. These topologies can achieve continuous operation even if a complete loss of one of the converter legs has happened, providing the global objective i. e. THD below 5%.
The power switch failure is compensated by reconfiguring the converter topology using connecting bi-directional devices and fuses. In the case of the topology τ_2, the faulty leg is replaced by a redundant one. In the case of the topology τ_1, the faulty leg is isolated. Then, the corresponding phase is connected to the middle point of the capacitor C_{dc}.

When comparing both topologies, we demonstrated that, in faulty case, performances can be guaranteed for each of them. Topology τ_1 does not need a redundant leg but however requires a higher dc-bus reference voltage to preserve the main performance features after fault compensation.

A Fault Tolerant Control (FTC) strategy dedicated to an active power filter which incorporates reliability analysis into the reconfigurable control structure selection has been also presented in this paper. Once a fault occurred, the proposed FTC strategy will switch to the suitable structure. The selected structure will guarantee an optimal performance of the reconfigured system according to the "highest" reliability in order to ensure the dependability of the active power filter system.

REFERENCES

[1] Kastha, D.;Bose, B.K., "Investigation of fault modes of voltage-fed inverter system for induction motor drive", *IEEE Transactions on Industry Applications*, Vol. 30, Issue 4, July-August 1994 pp. 1028–1038.

[2] Thybo, C., "Fault-tolerant control of induction motor drive applications", *American Control Conference, 2001. Proceedings of the 2001*, Vol. 4, 25-27 June 2001, pp. 2621 – 2622.

[3] De Araujo Ribeiro, R.L.; Jacobina, C.B.; da Silva, E.R.C.; Lima, A.M., "Fault detection of open-switch damage in voltage-fed PWM motor drive systems", *IEEE Transactions on Power Electronics*, Vol. 18 , Issue: 2 , March 2003, pp. 587 – 593.

[4] Beltrao de Rossiter Correa, M.; Brandao Jacobina, C.; Cabral da Silva, E.R.; Nogueira Lima, A.M., "An induction motor drive system with improved fault tolerance", *IEEE Transactions on Industry Applications*, Vol. 37, Issue 3, May-June 2001, pp. 873 – 879.

[5] Jacobina, C.B.; Correa, M.B.R.; Pinheiro, R.F.; Lima, A.M.N.; da Silva, E.R., " Improved fault tolerance of active power filter system", *Power Electronics Specialists Conference*, 2001. PESC. 2001 IEEE 32nd Annual , Vol. 3, 17-21 June 2001.

[6] Jacobina, C.B.; Pinheiro, R.F.; de R. Correa, M.B.; Lima, A.M.N.; da Silva, E.R.C., "Control of a three-phase four-wire active filter operating with an open phase", *Industry Applications Conference, 2001. Thirty-Sixth IAS Annual Meeting. Conference Record of the 2001 IEEE*, Vol.: 1, 30 Sept.-4 Oct. 2001.

[7] Zhang, Y.M. and J. Jiang, "Bibliographical review on reconfigurable fault-tolerant control systems", *IFAC Safeprocess, 2003, Washington DC, USA.*

[8] Staroswiecki, M., G. Hoblos and A. Aitouche, "Sensor network design for fault tolerant estimation", *Int. J. Adapt. Control Signal Process, 2004*, vol. 18, pp.55-72.

[9] Guenab F., D.Theilliol, P.Weber, J.C.Ponsart and D.Sauter, "Fault tolerant control method based on costs and reliability analysis", *16th IFAC World Congress*, Prague,2005, Czech Republic.

[10] Wu, N. Eva, "Reliability of fault tolerant control systems", Part I. *IEEE Conference on Decision and Control, 2001, Orlando, Florida, USA.*

[11] Wu, N. Eva. and Ron J. Patton, "Reliability and supervisory control", *IFAC Safeprocess, Washington DC, 2003, USA*, pp. 139–144.

[12] Bobbio A., "Dependability analysis of fault-tolerant systems: a literature survey", *Microprocessing and Microprogramming*, 1990, vol. 29, pp. 1-13.

[13] Bobbio A., "Architectural factors influencing the reliability of fault-tolerant VLSI arrays", *Microelectronics and Reliability*, 1990, vol. 31, pp. 963-968.

[14] H. El Brouji, P. Poure and S. Saadate, "Study and comparison of fault tolerant shunt three-phase active filter topologies", *IEEE 5th International Power Electronics and Motion Control Conference*, 13-16 August, 2006 Shanghai, P.R.China.

[15] H. Akagi, Y. Kanazawa, A. Nabae, "Generalized theory of the instantaneous reactive power filter", Proceeding *International power electronics conference*, Tokyo, Japan, pp. 1375-1386, 1983.

[16] H. S. Song, "Control scheme for PWM converter and phase angle estimation algorithm under voltage unbalanced and/or sag condition", PhD in Electronic and Electrical Engineering, POSTECH university, republic of Korea (south), 2001.

[17] Ansell, J.I. and Phillips M.J., "Practical methods for reliability data analysis", 1994, Oxford University Press Inc, ISBN 0 19 853664 X, New York.

[18] Lu, Z. and Liu W., "Reliability evaluation os STATCOM based on the k-out-of-n: G Model", 2006

International Conference on Power Systems Technology, Oct. 2006, pp. 1-6.
[19] Tippachon W., Boonruang R., Khamtang C., Klairuang D., Rerkpreedapong J., Hokierti J., “Failure analysis of protective devices in power distribution systems for reliability analysis purpose”, TENCON 2006, IEEE Region 10 Conference, 14-17 Nov. 2006, pp. 1-4.
[20] Horton, W.F. and Goldberg S., “The failure rates of overhead distribution system components”, 1994, Proceedings of the 1994 IEEE Power Engineering Society, 22-27 Sept. 1994, pp. 713-717.